rijksuniversiteit
groningen

Erasmus Mundus Master in Theoretical Chemistry and Computational Modeling

Theoretical study of hole and electron transfer in *p*-quinquephenyl dimers: A conformational analysis

Luis Enrique Aguilar Suárez

S3008002

Supervisors

Remco W. A. Havenith
Daniel Roca Sanjuán
Ria Broer

Abstract

Organic electronics is the field concerning the design, synthesis, characterization and application of small organic molecules with electronic properties, e.g. conductivity. These materials present desirable advantages over inorganic semiconductors, such as flexibility, thermal stability, low cost and lightweight. Thus, the search of new materials becomes a priority in this field.

Hole and electron transfer are key processes to be studied in a new material due to they drive most of the electronic properties; these processes are strongly influenced by the mutual orientation of the molecules. Among small organic molecules, *p*-quinquephenyl is a promising material since it is the simplest rod-like molecule able to be present in three different phases: crystal, liquid crystal and liquid.

The aim of this project is to determine how the hole and electron transfer are influenced by different orientations of the *p*-quinquephenyl molecules in the liquid crystalline phase; in this phase, the oligomer could be used in a wide range of applications, such as organic semiconductors, light emitters and organic dielectrics. For that, we performed a theoretical study using *p*-quinquephenyl dimers determining the electronic coupling at different values of distances of separation, displacements and rotations.

Our results show that charge transfer exists in the liquid crystalline phase of *p*-quinquephenyl and it is preferably a hole conductor in most of the configurations. High electronic coupling values arise from the parallel displacements of the molecules; these movements are exclusively allowed in the liquid crystalline phase. The results suggest that rotations do not play an important role in the hole transfer.

According to our results, the hole transfer is enhanced in the liquid crystalline phase when compared with the crystalline phase, whereas it is almost non-existing in the liquid phase due to high distances of separation and free rotations of the monomers.

Table of Contents

Introduction

Optoelectronics: Looking for new materials

Optoelectronics is the field of science materials devoted to the design, the synthesis, the characterisation and the application of small organic molecules that show desirable electronic properties in electronic devices [1, 2], such as organic field-effect transistors (OFETs), organic light-emitting diodes (OLEDs), or in organic photovoltaics (OPVs) [3, 4]. Organic-based optoelectronic devices provide some advantages over inorganic-based ones, such as flexibility, lightweight, thermal stability to operate at high temperatures, low cost of fabrication and the possibility to grow large-area films that can be used in large-size devices. Despite the fact of the advantages that organic electronics offer due to their structural diversity, there are some challenges that must be overcome, such as low electron and hole mobility and the lack of knowledge of the relation between the electronic properties and the structural arrangement [4].

One of the tasks of optoelectronics is the search of new organic materials that can be implemented in optoelectronic devices. It is desired that these materials present high electron/hole mobility and these can be achieved by increasing the π overlap between neighbouring molecules. The packing in organic materials has been categorized in four types depicted in Figure 1; a) herringbone (face-to-edge); b) herringbone ($\pi - \pi$ overlap): c) lamellar 1-D stacking; and d) lamellar 2-D stacking. It is believed that the lamellar 2-D staking show the highest orbital overlap between neighbouring molecules, whereas the herringbone (face-to-edge) arrangement is believed to have the lowest orbital overlap of the four configurations [5].

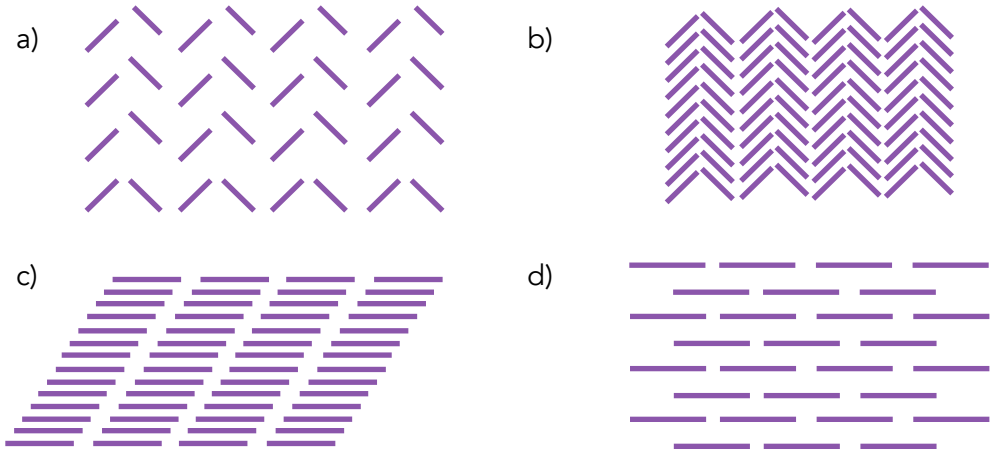

Figure 1. Typical molecular packing in organic crystals: a) herringbone (face-to-edge); b) herringbone ($\pi - \pi$ overlap): c) lamellar 1-D stacking; and d) lamellar 2-D stacking.

The electronic properties of an organic material arise from the charge transfer process, and the latter is strongly influenced by the intermolecular interactions and the mutual orientation between the molecules (i.e. the molecular packing that the material adopts) [6]. Thus, the study of charge transfer in an organic material is essential to determine how efficient that material would be for optoelectronic applications.

Charge transfer process in organic materials [7]

Initially described in ions in aqueous solution, the charge transfer process is a mechanism in which an electron is transferred between two entities (ions or organic molecules). For example, consider the following reactions between ions in solution

$$Fe^{2+}(aq) + Fe^{3+}(aq) \rightarrow Fe^{3+}(aq) + Fe^{2+}(aq)$$
$$Ce^{3+}(aq) + Ce^{4+}(aq) \rightarrow Ce^{4+}(aq) + Ce^{3+}(aq)$$
$$Fe^{2+}(aq) + Ce^{4+}(aq) \rightarrow Fe^{3+}(aq) + Ce^{3+}(aq)$$

These reactions represent the exchange of an electron between two units that are not necessarily the same. Rudolph Marcus called these exchange processes the simplest class of reactions that can be found in chemistry, mainly for two reasons:

a. The products and the reactants are the same in the charge transfer reaction; this fact leads to the elimination of the thermodynamic stability of the reactants and the products that usually influences the reaction rate.
b. There is no bond breaking or bond formation during the charge transfer process; rather, there is simply an electron exchange.

In contrast with ions in aqueous solutions, the transfer in organic materials (e.g. oligomers, polymers, etc.) is not limited to electrons, additionally holes and excitons are also able to be transferred between the organic units [8]; it is generally accepted that the charge transfer takes place by means of a so-called "hopping" process, which means that the electrons are transferred sequentially from the anionic form of a molecule to a neighbouring neutral one through the LUMO for the case of electron transport, and electrons are sequentially transferred from the neutral form of a molecule to the cationic form through the HOMO for the case of hole transfer [6]. Usually, efficient hole-transporting materials are those that present low ionisation potentials and low electron affinities, whereas high electron affinities and ionisation potentials are characteristics of efficient electron-transporting materials. It is worth to point out that a number of materials exhibit an ambipolar behaviour meaning that they are able to transport both electrons and holes with virtually the same efficiency (similar k_{CT}).

The charge transfer, for both electron and hole, is heavily dependent on the arrangement of the molecules and it is crucial for the application of new materials in optoelectronics devices. At a microscopic level, the mechanism of charge transfer can be described as the transport of an electron (or a hole) from a charged monomer to an adjacent neutral oligomer. In the limits of weak coupling, the charge (electron or hole) transfer rate (k_{CT}) can be approximated as [9]

$$k_{CT} = \frac{4\pi^2}{h\sqrt{4\pi k_B T}} V^2 exp(-\frac{\lambda}{4\pi k_B T}) \quad (1)$$

where λ is the reorganisation energy, that is the energy dissipated when a system that has undergone a "vertical" electron transfer relaxes to the equilibrium structure of the new charge distribution (Figure 2) , k_B is the Boltzmann constant, T is the temperature, h is Planck's constant and V is known as the electronic coupling term [10].

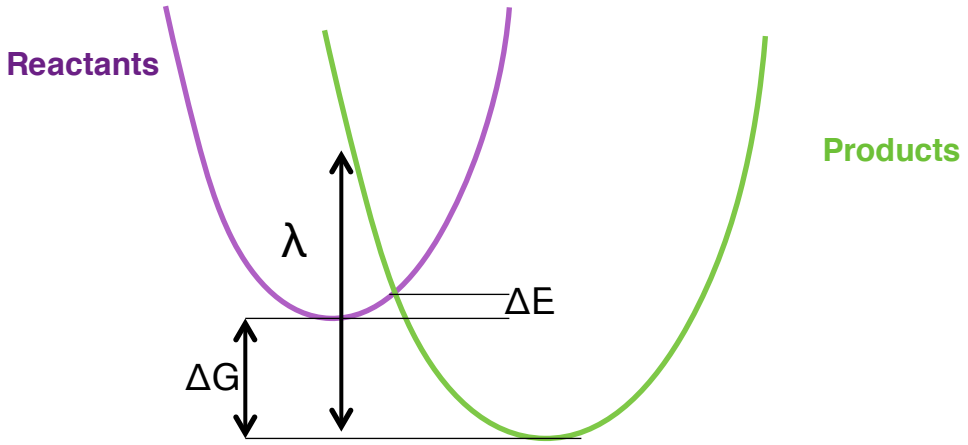

Figure 2. Potential energy surface for reactants and products; λ is the reorganisation energy, ΔE is the activation energy and ΔG is the free energy change between the reactants and the products.

Determination of V: Direct coupling scheme

V expresses how easy the transfer of a charge (hole or electron) is between two interacting entities and it is the key parameter that controls the absolute k_{CT} in a material. V can be obtained directly by means of the so-called direct coupling (DC) scheme [11]. In this scheme, only the initial and the final states of a dimeric system are taken into account [12]. Considering the hypothetical dimer A-B, in the charge transfer process the initial state corresponds to that in which the electron (or hole) is located in molecule A while B remains neutral, whereas the final state corresponds to that one in which now the electron (or hole) is located in monomer B and monomer A stays neutral [11]. The determination of how V is influenced at a molecular level by the different orientations of the interacting molecules is crucial to understand the transport properties in new materials. V is usually calculated within the DC scheme and can be expressed as half of the energy difference between the two states:

$$V = \frac{H_{if} - \frac{(E_i + E_f)\cdot S_{if}}{2}}{1 - S_{if}^2} \quad (2)$$

where E_i and E_f are the energies of the initial and final state of the system, respectively, and they can be defined as $E_i = \langle \Psi_i | \hat{H} | \Psi_i \rangle$ and $E_f = \langle \Psi_f | \hat{H} | \Psi_f \rangle$, whereas the overlap integral between the two states (S_{if}) is defined as $S_{if} = \langle \Psi_i | \Psi_f \rangle$ and $H_{if} = \langle \Psi_i | \hat{H} | \Psi_f \rangle$ is the matrix element of the Hamiltonian. When the diabatic wave functions of the initial and final states (a diabatic state does not change its physical character as one moves along the reaction coordinate) are not orthogonal to each other, there is an overlap contribution for the coupling [13, 14].

The determination of V and how the molecular packing influences it are essential for any material that is intended for optoelectronic applications.

The new material: *p*-quinquephenyl

Poly-*p*-phenylene (PPP) oligomers are organic molecules that have attracted a lot of attention due their unique behaviour as rigid-rod molecules [15]. Rigid-rod molecules are rod-shape molecules that cannot be bent or compressed, and their applications have gained a lot of interest especially in the field of material sciences as part of optoelectronic devices. However, the electronic properties for most of the PPP oligomers remain experimentally and theoretically unknown. In this project, we focus our attention on *p*-quinquephenyl (PQP). PQP (Figure 3) is the simplest rigid-rod-like molecule [15] and its study might provide a deep insight in the behaviour of more complex rigid-rod molecules.

Figure 3. Depiction of the structure of a *p*-quinquephenyl monomer; the molecule under study in this project

PQP is an interesting material as it can be present in a liquid crystalline phase. Dingemans *et al.* [16, 17] have determined the specific transition temperatures between the crystal (K) to the liquid crystalline phase (N) and from the N to the liquid phase (I) of the PQP; the transition temperatures are specified in Table 1.

Table 1. Transition temperatures of the different phases of PQP

Transition temperatures (K)	
K → N	666
N → I	698

The experimentally determined crystalline structure of PQP corresponds to a herringbone (face-to-edge) packing [18, 19]; for this system it was determined that the average distance of separation between the monomers is 3.5 Å [20]. A Molecular Dynamics (MD) [21] study shows the different arrangements of PQP in the crystalline (Figure 4), liquid crystalline and liquid phases. In the crystalline phase, the oligomers are oriented in a herringbone configuration, whereas in the liquid crystalline phase the oligomers are packed in a lamellar 2-D configuration, in which the oligomers of PQP are allowed to rotate, displace and separate. Contrary to the experimental determination, the average distance of separation between the oligomers is 5.5 Å in the MD simulations. In the liquid phase, as expected, the molecules present a complete random orientation.

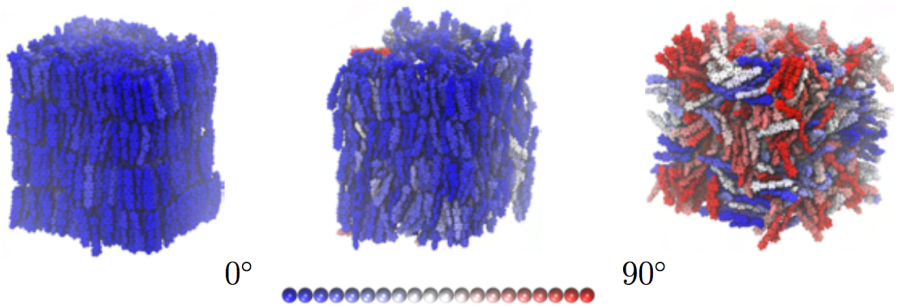

Figure 4. MD snapshots of the different phases; herringbone configuration at crystalline phase (left); lamellar 2-D configuration at liquid crystalline phase (center) and random orientation in liquid phase (right). Taken and adapted from Ref [21] Copyright 2014 Wiley-VCH Verlag GmbH & Co. KGaA, Weinheim

There is no data available of the electronic properties of PQP in the liquid crystalline phase owing to the range of temperature is too high (above 391°C) making it difficult to study it experimentally. However, the study of PQP is essential to clarify more complex rod-like systems in the liquid crystalline phase. We performed a theoretical study to determine how the hole, electron and exciton transfers are influenced by the different conformational arrangements in a PQP dimer.

Complete Active Space Self-Consistent Field [22, 23]

One of the approaches (explained in Computational details) to obtain the elements required in (2) for the computation of V is based in the generation of antisymmetrized product functions of the monomers, and the latter wave functions can be generated through the Complete Active Space Self Consistent Field (CASSCF) method. CASSCF is a multiconfigurational method used in quantum chemistry to describe systems in cases where Hartree-Fock and density functional theory are not adequate. In the CASSCF approach, the orbitals of the system are divided in three spaces (Figure 5): 1) an inactive space, in which the orbitals are doubly occupied, 2) an active space, in which the orbitals are allowed to be partially occupied, and 3) a virtual space consisting of orbitals that must have zero electrons.

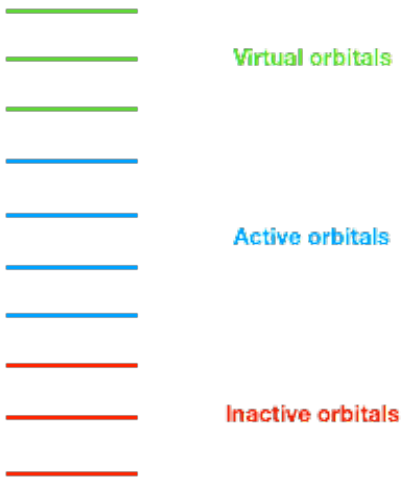

Figure 5. Depiction of the three spaces in which the orbitals are divided within the CASSCF approach; the inactive orbitals are doubly occupied, whereas the active orbitals can be partially occupied and the virtual orbitals must contain zero electrons

The configuration state functions (CSFs) in the CASSCF calculations, which are symmetry-adapted linear combinations of Slater determinants, are configurations that arise from all the possible ways of distributing all the active electrons (those electrons that are not included in the occupied orbitals) over the active orbitals in the appropriate combination (correct number of electrons, spin, and appropriate spatial symmetry); this is known as a full configuration interaction (FCI). A FCI expansion is constructed from those CSFs and the CASSCF wave function is obtained by optimizing the coefficients and the orbitals in (3)

$$\Psi_s = \sum_{J=1}^{L} C_J \Psi_J \quad (3)$$

The selection of which orbitals are included in the active space is crucial for the CASSCF calculations. One of the main drawbacks of the CASSCF methodologies is that the number of CSFs scales factorially with the number of active orbitals and the number of electrons. Therefore, in practice, the number of orbitals and electrons are limited by computational power.

Computational details

The approach hereby used to determine the electronic coupling between the initial and final diabatic states by using a nonorthogonal configuration interaction is reported somewhere else [24]. This method is closely related to the approach used for the calculation of correlated many-electron bands [25].

The approach is based in the construction of antisymmetrized product functions of the monomers. Therefore, the wave functions and the orbitals of the cation (Ψ_{PQP^+}), the anion (Ψ_{PQP^-}) and the neutral form (Ψ_{PQP}) of PQP were obtained using CASSCF(4,4) calculations (ANO-L basis set for C and H) using the MOLCAS 7.4 software [26]. Then a dimer was constructed to study the hole transport as follows: the orbitals of the cationic form of PQP were projected on the basis of the dimer, and were combined with the orbitals of the neutral form that were also projected in the basis of the dimer. Then the orbitals of the dimer were used in CASCI(8,8) calculations and the resulting wave function is the many-electron basis function (MEBF) describing the initial state (in which one of the monomers is ionised). The eight orbitals in the active space of the dimer for the CASCI calculation correspond to the active orbitals in the previous monomer calculations. The MEBF describing the final state was constructed similarly following the procedure described above, but for this case the first monomer is in the neutral form, whereas the second one is a cation. Taking a simple dimer of PQP molecules labelled as A and B, the initial and final states can be expressed as

$$\Psi_i = \Psi_{A^+ \cdot B} = \mathbf{A}\Psi_{A^+}\Psi_B \quad \text{(Initial state)}$$
$$\Psi_f = \Psi_{A \cdot B^+} = \mathbf{A}\Psi_A\Psi_{B^+} \quad \text{(Final state)}$$

where $\mathbf{A}$ is an antisymmetrizer.

The Hamiltonian and overlap matrix elements between the MEBFs required for the determination of V (Equation 2) were obtained using the RASSI program of MOLCAS.

For the electron transport, the same methodology was used to construct the dimer [27], but the anionic form of PQP was used instead of the cationic form. The initial and final states, then can be written as

$$\Psi_i = \Psi_{A^-.B} = \mathbf{A}\Psi_A{}^-\Psi_B \text{ (Initial state)}$$
$$\Psi_f = \Psi_{A.B^-} = \mathbf{A}\Psi_A\Psi_B{}^- \text{ (Final state)}$$

Advantages of this method, described by Havenith, de Gier and Broer, is that it provides a clear chemical interpretation of the initial and final states in molecular MEBFs, and the wave function is compact in case of orbital changes and multi-reference character in the different states.

Conformational parameters studied

The electronic couplings were evaluated for different distances of separation between the monomers, for different displacements and different rotations as explained below

Distances of separation

The V of a dimer was evaluated at different distances of separation in the range 2.5-10.5 Å in steps of 1.0 Å (Figure 6). Displacements and rotations were evaluated at different distances of separation; 3.5Å (experimental $\pi - \pi$ distance of separation), 5.5Å (theoretical MD $\pi - \pi$ distance of separation) and 4.5Å (average value between the experimental and theoretical values).

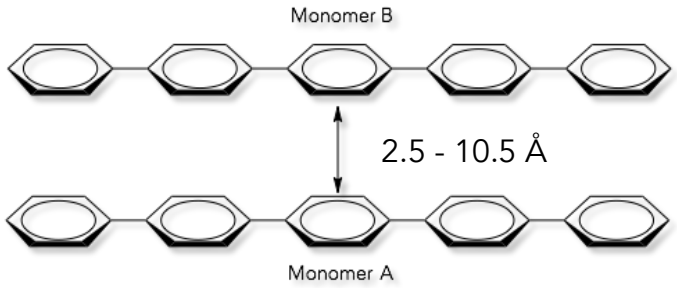

Figure 6. Distances of separation studied between the monomers in the PQP dimer.

Displacements

To evaluate the influence of the different displacements in the V the cofacial conformation of the dimer was taken as the starting point. As depicted in Figure 7, monomer A was fixed to its original position while monomer B was displaced along its long molecular axis from 0 Å (cofacial conformation) to 18 Å in steps of 1.0 Å.

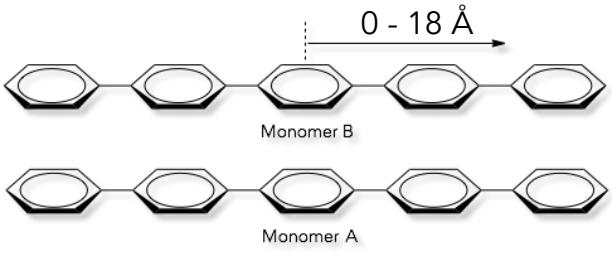

Figure 7. Displacements of the monomer B in the PQP dimer

Rotations

To evaluate the influence of the rotations at the different distances of separation, the cofacial conformation of the dimer was taken as the starting point. As depicted in Figure 8, monomer A was fixed to its original position while monomer B was rotated over its long-molecular axis from 0°(cofacial conformation) to 90° (perpendicular configuration) in steps of 10°.

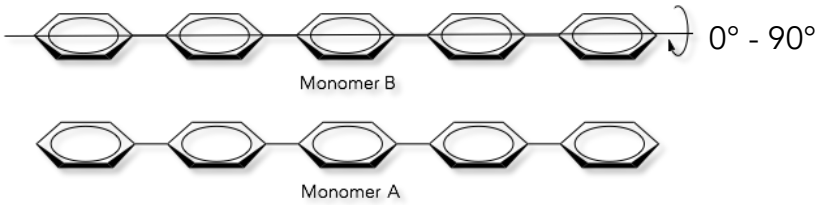

Figure 8. Rotations of the monomer B in the PQP dimer

Aim

Determine theoretically how the spatial arrangement at different distances of separations, different displacements from the cofacial configuration and different rotations affect the electron and hole transfer in the liquid crystalline phase of PQP by quantifying the electronic coupling. Besides that, it will be determined: 1) how the random spatial arrangement of PQP molecules affects the electron and/or hole mobility in the liquid phase and how it differs from the crystalline phase, and 2) for the liquid crystalline phase it will be determined if electron and/or hole mobility exists and how it differs from the crystalline structure.

Results and discussion

Preliminary considerations

Active Space

Due to the quasi-degeneracy of the orbitals in PQP (Figure 9), an active space of 4 electrons in 4 orbitals was selected for the CASSCF calculations in the monomer. From the simple Hückel molecular orbital diagram (Figure 9) it can be concluded that the 6 (quasi) degenerated orbitals (HOMO-2 to HOMO-7) either are included in the CASSCF calculations of the monomer or not included at all; if the degenerated orbitals are included this will lead to CASSCF(16,16) calculations for the monomer, and subsequently CASCI(32,32) calculations for the dimer that are not currently computationally affordable. Therefore, an active space of 4 electrons in 4 orbitals was selected for the calculations of the monomer.

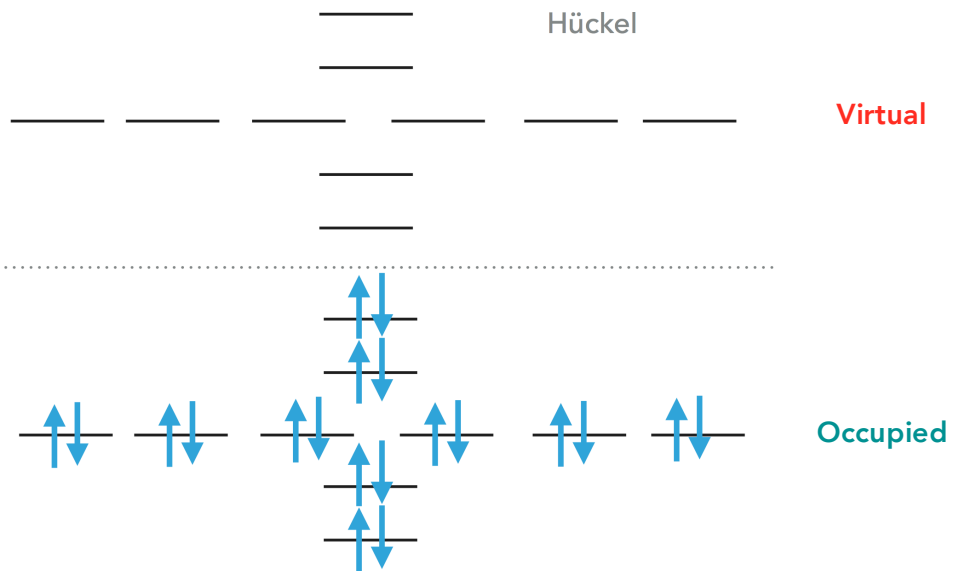

Figure 9. Diagram of π energy levels of the PQP monomer calculated with the Hückel method

Ionisation potentials

Due to the quasi-degeneracy of the highest occupied orbitals in PQP, the ionisation potential of PQP was calculated for two different situations in order to determine from which orbital the electron is removed and use it in the CASSCF(4,4) calculations: 1) the electron is removed from HOMO-1; and 2) the electron is removed from HOMO. The results are shown in Table 2.

Table 2. Calculated ionisation potentials of PQP

Orbital	Irreducible representation	IP (eV)
HOMO (Calculated)	$^1B_{2g}$	6.84
HOMO-1 (Calculated)	$^1B_{1u}$	6.53

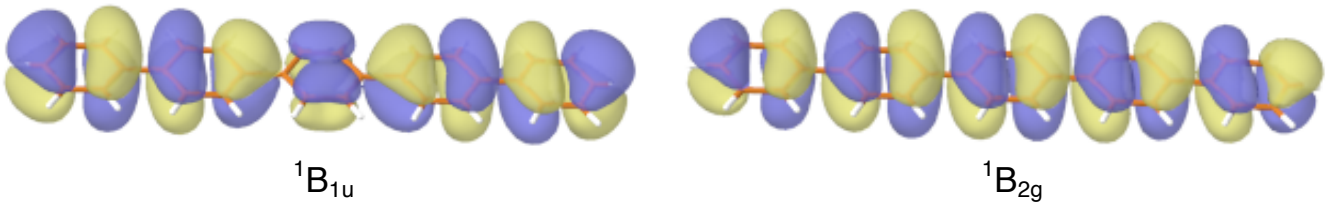

Figure 10. Schematic representation of HOMO-1 (*left*) and HOMO (*right*) of the PQP molecule; the irreducible representations of each orbital is indicated.

The total energy of the ionized form shows that when the PQP monomer is ionized from the HOMO-1 (E = -1149.18804236 a.u.) the resulting cation is more stable than the cation formed when the PQP is ionized from the HOMO (E = -1149.17664973 a.u.). Therefore, the HOMO-1 was selected as the ionized orbital for all the calculations.

Electronic coupling in the crystalline phase

The electronic coupling in the crystalline phase was calculated using the same methodology described in the computational details. A dimer was constructed from the experimental herringbone structure of PQP [18], the selected dimer from the structure is circled in blue in Scheme 1. The calculated V for the dimer is 150 mV; this value is taken as a reference for the crystalline structure.

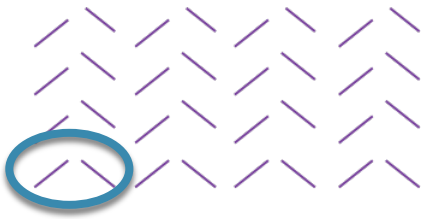

Scheme 1. Herringbone (face-to-edge) packing of the crystalline structure of PQP; the taken dimer for the study is circled in blue

Dimer

Hole

Distances of separation

The electronic coupling for the hole transfer at different distances of separation and the corresponding orbital overlap are shown in Figure 11.

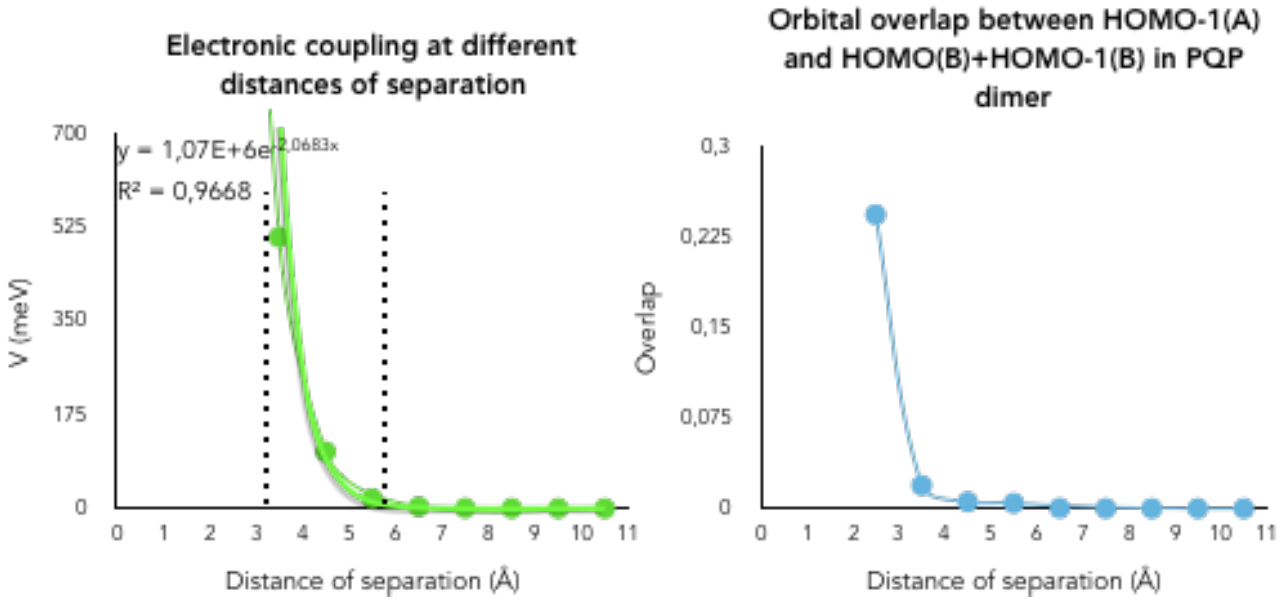

Figure 11. Electronic coupling (hole) and orbital overlap at different distances of separation in a PQP dimer; V at 2.5 Å is not plotted for clarity of the exponential fitting

There is an exponential decay of the V values as the distance of separation is increased; the exponential fitting is shown in Figure 11. At the shortest distance of separation (2.5 Å) V=2.24 eV but the point was not plotted in Figure 11 for clarity of the exponential fitting.

The orbital overlap between the HOMO-1 (hole-containing orbital) of the cation form and the HOMO and HOMO-1 of the neutral molecule was determined in order to understand the exponential decay of the V. The orbital overlap values are shown in Figure 11; it can be established that the electronic coupling depends on the orbital overlap for the different distances of separation. For the liquid crystalline phase, the V values are expected to be in the range of 3.5 (experimental distance of separation) - 5.5 Å (theoretical distance of separation), such zone is highlighted in Figure 11. It is worth to mention that the V becomes zero at distances of separation higher than 6.0 Å, indicating that hole transfer is not enhanced in the liquid phase of PQP since the molecules are randomly oriented with distances of separation between the molecules higher than 6.0 Å.

In order to corroborate the underlying cause of the V decreasing, the overlap between the MEBFs (S_{ij}) was obtained at each distance of separation. These values are shown in Figure 12.

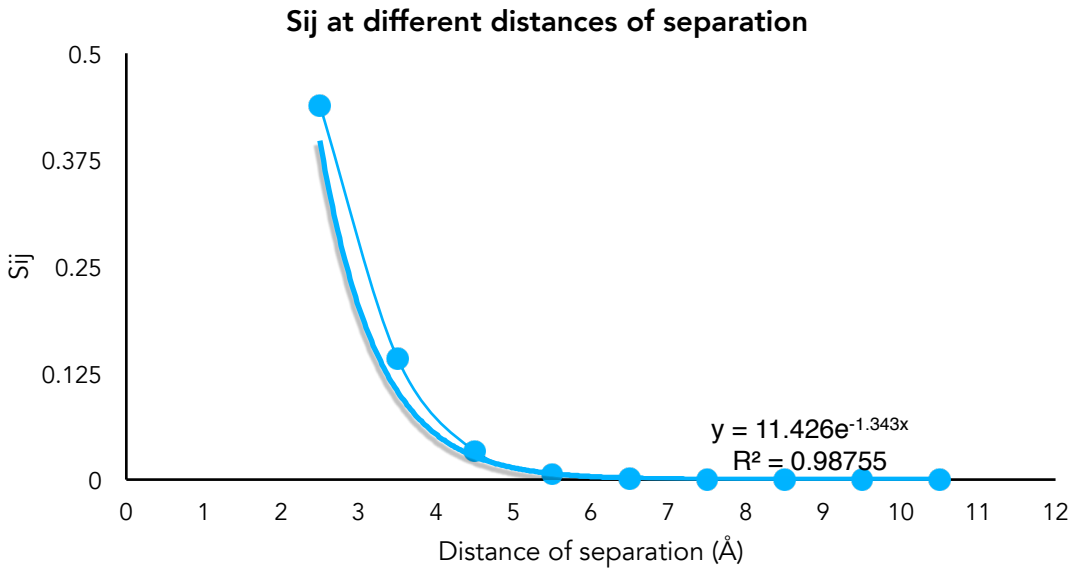

Figure 12. S_{ij} values at different distances of separation for PQP dimer; an exponential decay is observed when increasing the distance of separation

As seen in Figure 12, the value of S_{ij} decreases exponentially similar to the orbital overlap. Therefore, it can be conclude that the overlap is responsible for hole transfer in the PQP dimer.

Rotations

The V values when one of the monomers in a PQP dimer is rotated from 0-90° at different distances of separation are depicted in Figure 13.

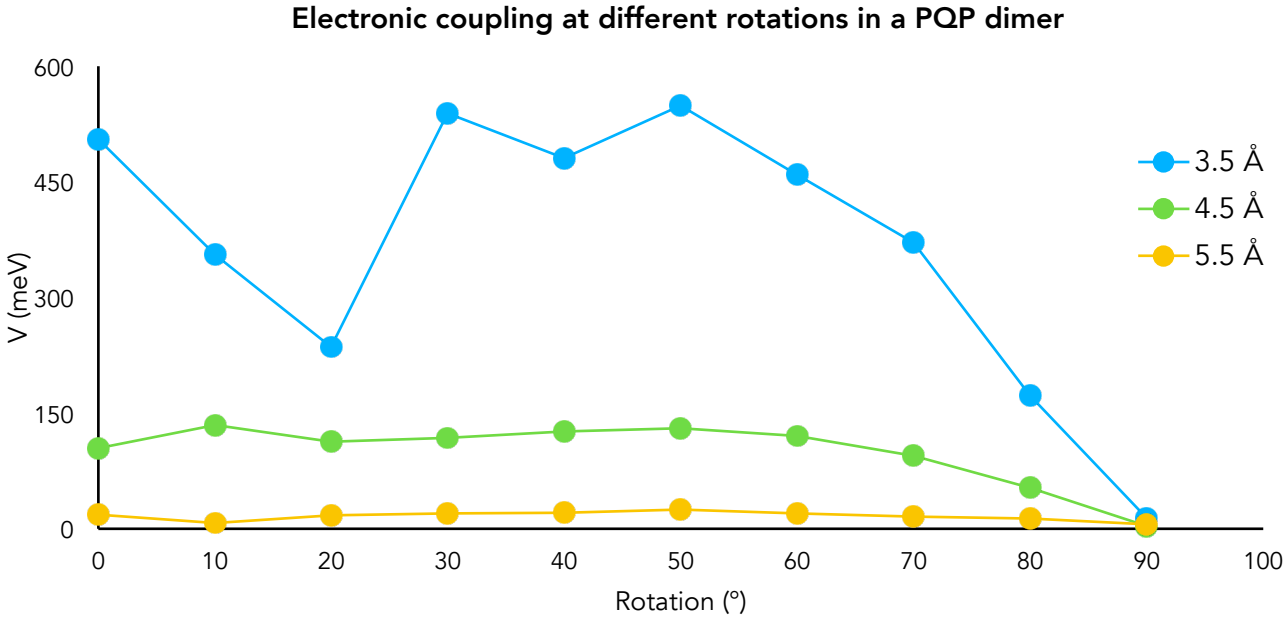

Figure 13. Electronic coupling in a PQP dimer when one of the monomers is rotated along its long molecular axis; for 3.5 Å the V decreases when the monomer is rotated, whereas at 4.5 and 5.5 Å the V remains rather constant for most of the rotations

From Figure 13 it can be concluded that for the shorter distance of separation (3.5 Å), only two rotations (30 and 50°) enhance the hole transfer, whereas the other configurations decrease the V.

It is worth to mention that V=0 at 90° for the three distances of separation; in this configuration the monomers are in a perpendicular position (Figure 14) in which the *p* orbitals do not overlap at all. Nevertheless, at 4.5 and 5.5 Å the V remains rather constant for a range of rotations between 10 and 60°; since only a few rotations are allowed in the liquid crystalline phase of PQP it is expected that the V remains constant in that range.

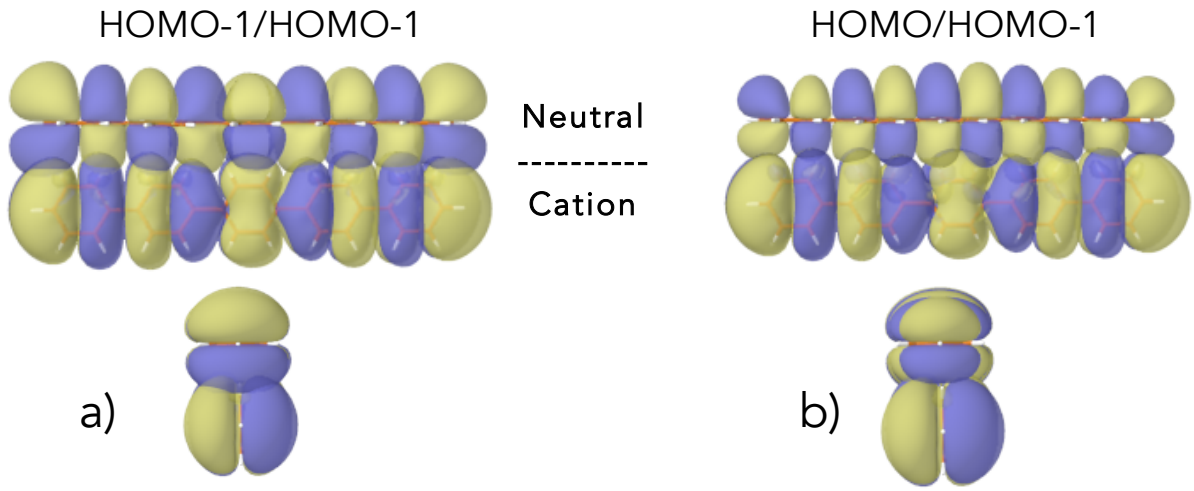

Figure 14. Orbital overlap between a) HOMO-1 of the cation and HOMO-1 of the neutral form, and b) HOMO-1 of the cation with HOMO of the neutral form when one of the monomers of the dimer has been rotated 90° over its long molecular axis. The perpendicular orientation of the orbitals leads to V=0

The orbital overlap between the HOMO-1 of the PQP cation with the HOMO and HOMO-1 of PQP neutral was obtained to explain the difference of V values at different rotations; the overlap values are depicted in Figure 15.

Figure 15. Orbital overlap between the HOMO-1 of in PQP cation with HOMO and HOMO-1 in the neutral PQP at different rotations; one of the monomers has been rotated along its long molecular axis. There is a decreasing in the V as the rotation is increased

For the case of hole transfer when one of the monomers is rotated, there is a correspondence between the HOMO overlap of the monomers and the V values; the higher the overlap, the higher the V value. It is worth to point out the decreasing V value in Figure 15 at 20° and 40°; in those specific configurations the HOMO overlap drops. A schematic representation of the decreasing of the HOMO overlap when increasing the rotation is depicted in Figure 16.

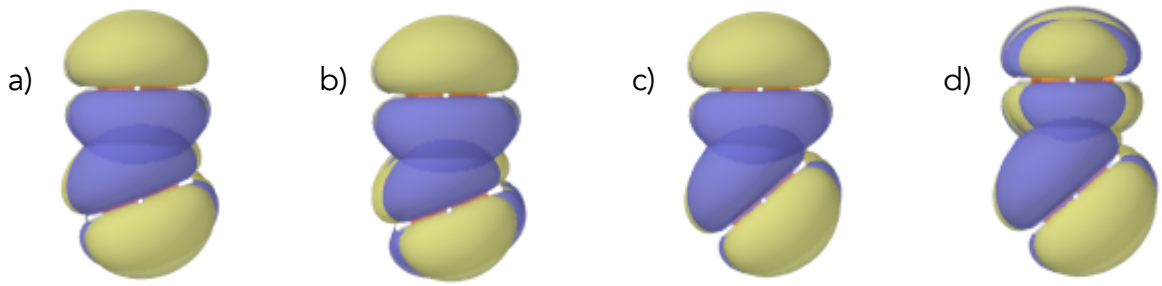

Figure 16. Orbital overlap between c) HOMO-1 (cation) and HOMO-1 (neutral) and d) HOMO-1(cation) and HOMO(neutral) at 20°; orbital overlap between c) HOMO-1 (cation) and HOMO-1 (neutral) and d) HOMO-1 (cation) and HOMO (neutral) at 40°

Rotations, which are allowed in the liquid phase of PQP, do not enhance the hole transfer when compared with the V calculated for the crystalline phase (150 meV). For the case of the liquid crystalline phase, some small rotations (up to 40°) might be allowed, but the V remains constant for most of the rotations (up to 70°) in the distant of separations 4.5 and 5.5 Å, therefore a change in the V because of rotations is not expected in this phase.

Displacements

Unlike the effect of rotating a monomer, in which there is a clear correspondence between the orbital overlap and the V, during the displacements evaluated at three distances of separation the V does not present a correspondence with the orbital overlap, i.e. the highest orbital overlap does not correspond to the highest V. From Figure 17, it could be inferred initially that the highest V values correspond to the 5 and 7 Å (Figure 18) displacements since in they have the highest overlap between the HOMO-1 of the cation with the HOMO and HOMO-1 of the neutral form. Even though the V values for both configurations are high (350 meV), there is another configuration showing a higher V. In Figure 18, the orbital overlap for both configurations is depicted. At a displacement of 5 Å there is a high overlap between the HOMO-1 of the cation and the HOMO-1 of the neutral form and an overlap between the HOMO-1 of the cation with the HOMO of the neutral form. The same behaviour is seen a displacement of 7 Å.

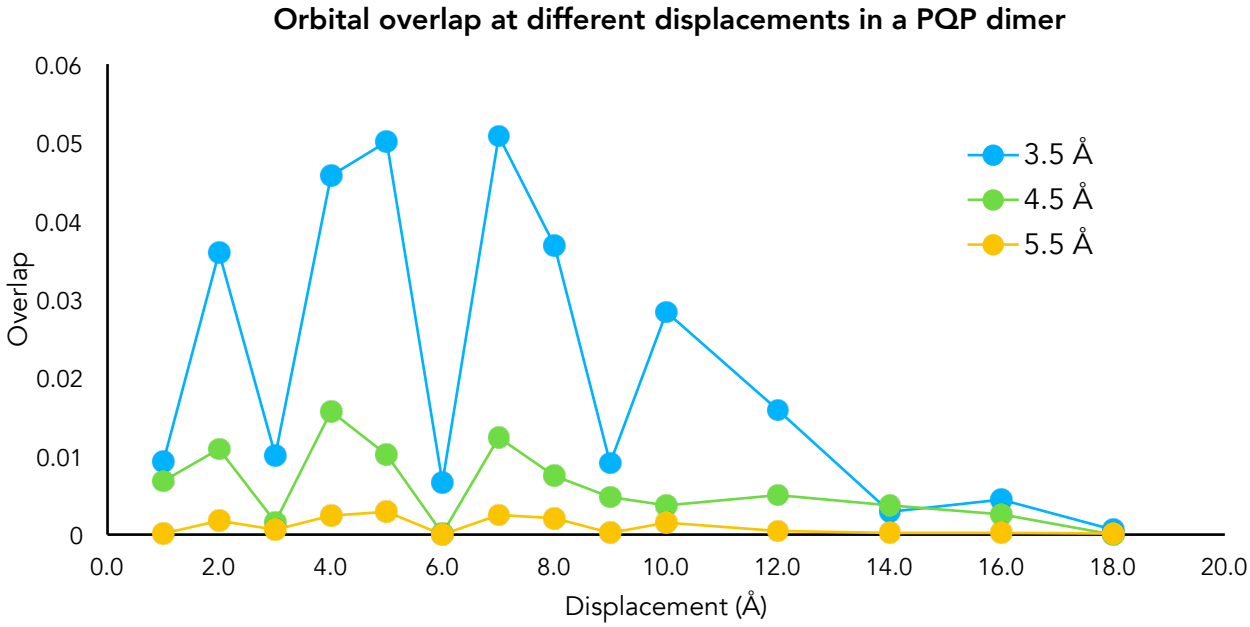

Figure 17. Orbital overlap between the HOMO-1 (cation) with HOMO and HOMO-1 (neutral) when one of the monomers is displaced along its long molecular axis in a PQP dimer at three different distances of separation

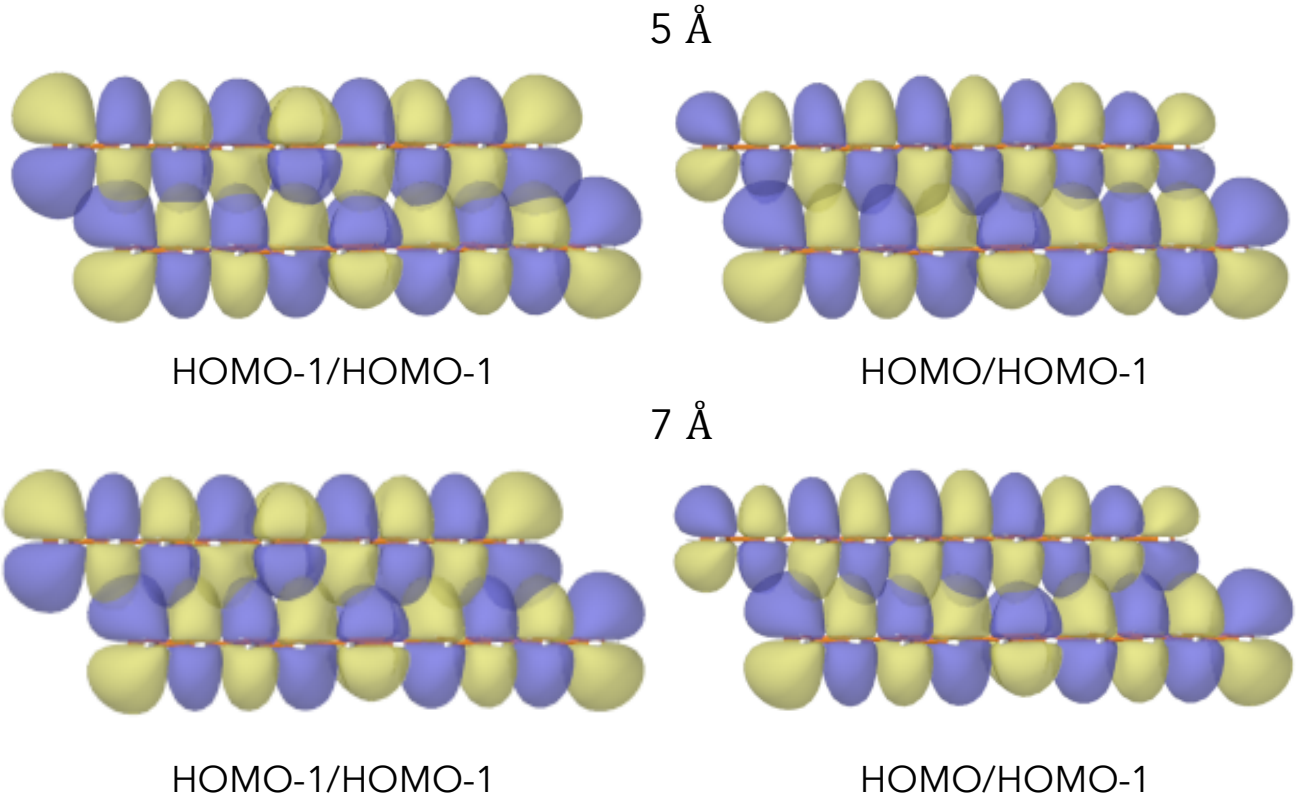

Figure 18. Orbital overlap between HOMO-1 of the cation (monomer at the bottom) and the HOMO and HOMO-1 of the neutral form (monomer on the top) in the configurations with the highest overlap values

The highest V value is observed at a displacement of 9 Å (Figure 17) independently from the distance of separation between the monomers. Therefore, the orbital overlap between the monomers is not enough to explain the different V values. Nevertheless, some other configurations can be explained based on the orbital overlap; for example, at 6 Å of displacement

there is a drastic decreasing of the V value in the three distances of separation evaluated. From Figure 17 we observe a drastic decreasing in the orbital overlap, which explains the behaviour in that particular point. Furthermore, the depiction of the orbital overlap shows that there is no a significant overlap between the HOMO-1 of the cation and the HOMO of the neutral form, and the existing HOMO-1/HOMO-1 overlap is smaller in comparison with the displacements at 5 and 7 Å. (Figure 20).

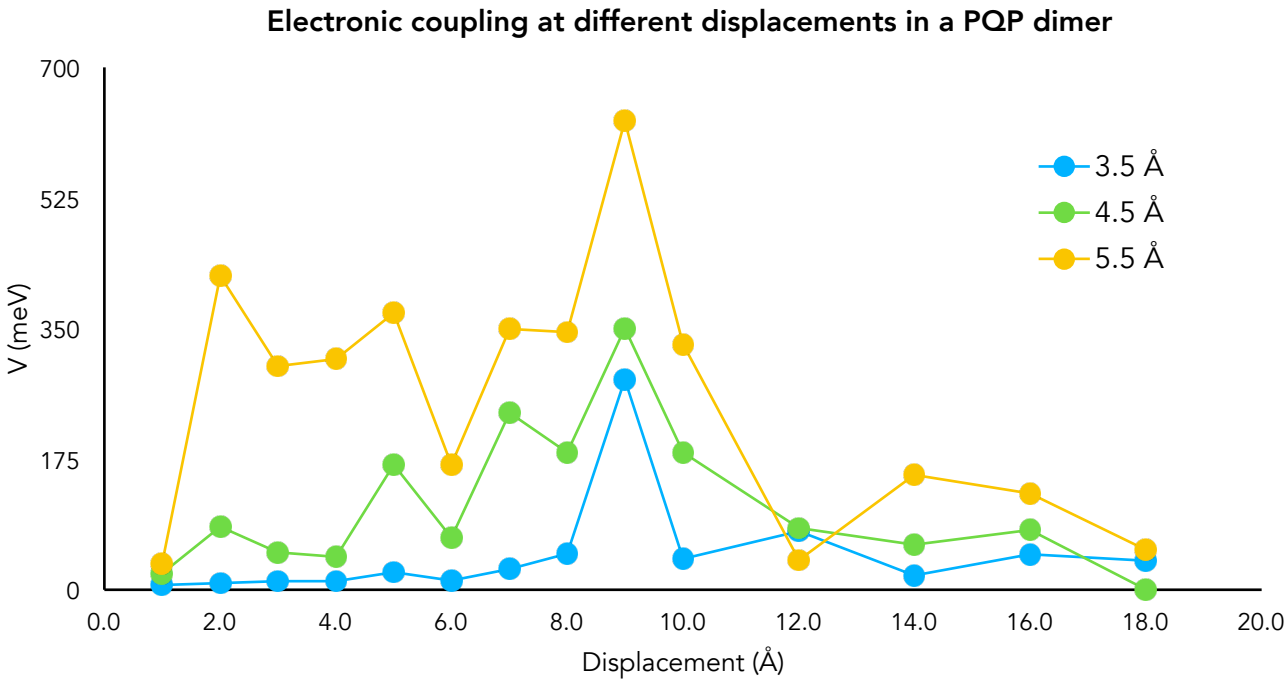

Figure 19. Electronic coupling at different displacements when of the monomers of PQP dimer is displaced along its molecular axis; for the three distances of separations studied, most of the configurations enhance the hole transfer

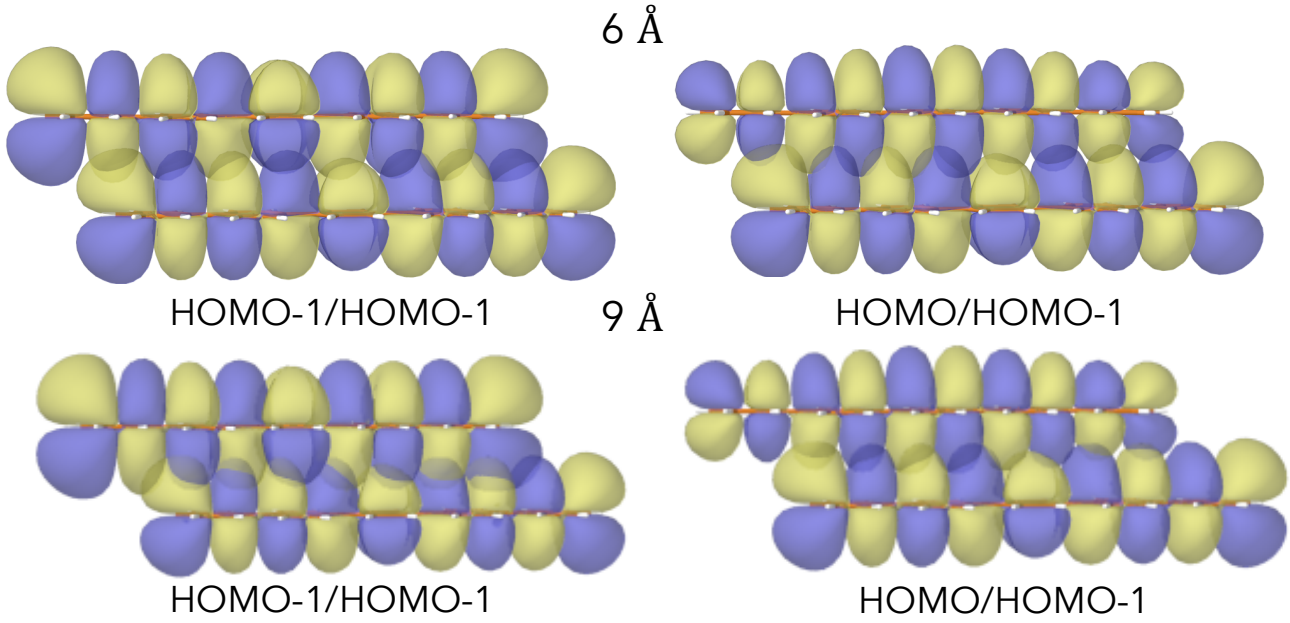

Figure 20. Orbital overlap at two displacements; the overlap between the HOMO-1 of the cation and the HOMO and HOMO-1 of the neutral form are depicted separately for each configuration

The total charge (Q) of each ring in the PQP cation was obtained from the individual Mulliken charges; the results are shown in Table 3; the charges of the neutral form of PQP are presented in Table 4.

Table 3. Total charges of the cationic form of PQP

Number ring	Q
1	0.12
2	0.24
3	**0.34**
4	0.19
5	0.11

Table 4. Total charges of the neutral form of PQ

Number ring	Q
1	0.00
2	0.01
3	-0.02
4	0.01
5	0.00

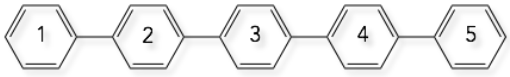

It was determined that the positive charge is located preferably in the centre ring (Number 3) of the PQP oligomer. For the case of the neutral form, there is no significant difference between the charges in the rings. Figure 19 represents the displacement at 9, in this particular configuration the ring in which the positive charge is preferably located (Ring number 3) is facing the ring in the neutral form that has a slightly negative charge; thus, it is believed that this direct overlap between the rings is the responsible of the high V, even tough the overall orbital overlap value is smaller than the one in the displacements at 5 and 7 Å. The decrease in the overlap can be explained in the sense that when the monomer is displaced, the orbitals in the extremes are not interacting with any other orbital. It can be concluded that, for the three distances of separation studied, some configurations arising from the parallel displacements enhance the hole transfer in the PQP dimer in comparison with the V calculated for the crystalline phase (150 meV). These parallel displacements are exclusively allowed in the liquid crystalline phase of PQP.

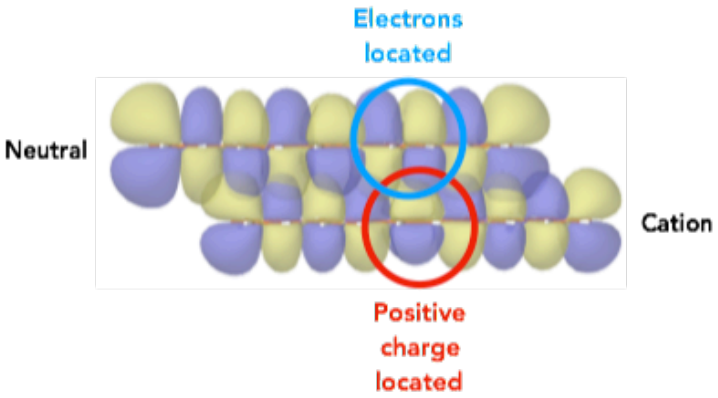

Figure 21. The positively-charged rings from the cation interacting with the ring of the neutral form of PQP; the configuration depicted is at a displacement of 9 Å of the cationic form

Electron

Distances of separation

The electronic coupling for the hole transfer at different distances of separation and the corresponding orbital overlap are shown in Figure 21.

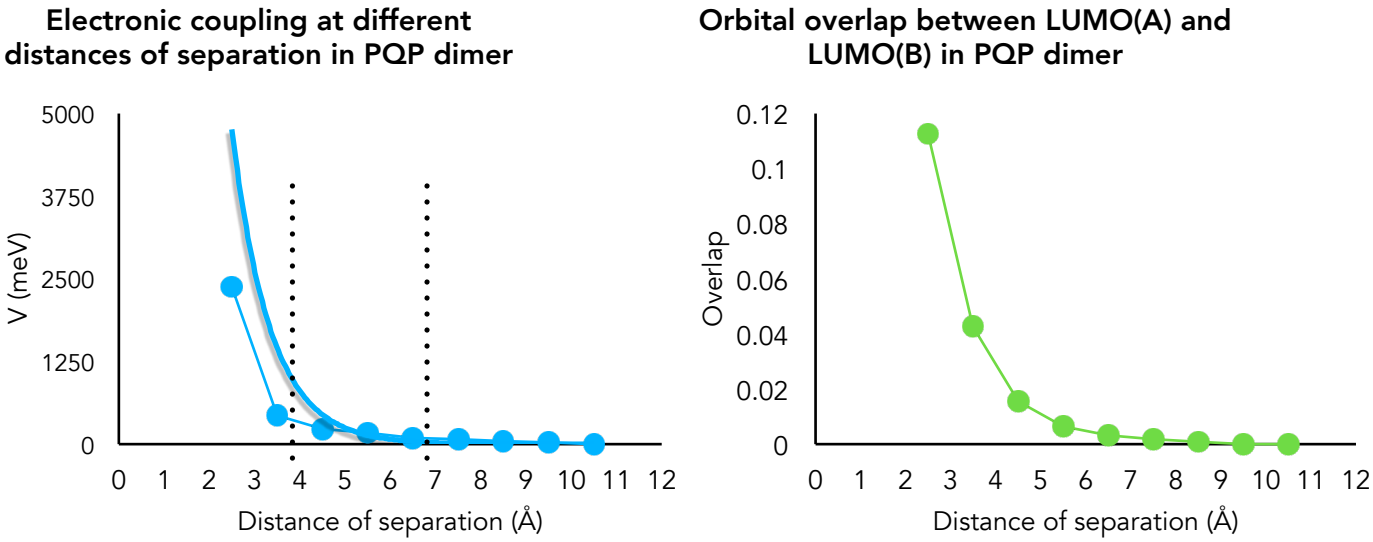

Figure 21. Electronic coupling (electron) and orbital overlap at different distances of separation in a PQP dimer where a decay of the V is observed.

From Figure 21 can be concluded that the efficiency of electron transport is reduced (i.e. decreasing of the V) when increasing the distance of separation between the monomers in the PQP dimer. Like the hole transfer behaviour, the depletion of the V can be attributed to the orbital overlap but in this case between the LUMOs of both monomers; the LUMO+1 was not included in the description because it does not contribute significantly to the overlap (overlap values = 0.0000). Unlike the hole, the electron transfer does not follow an exponential decay.

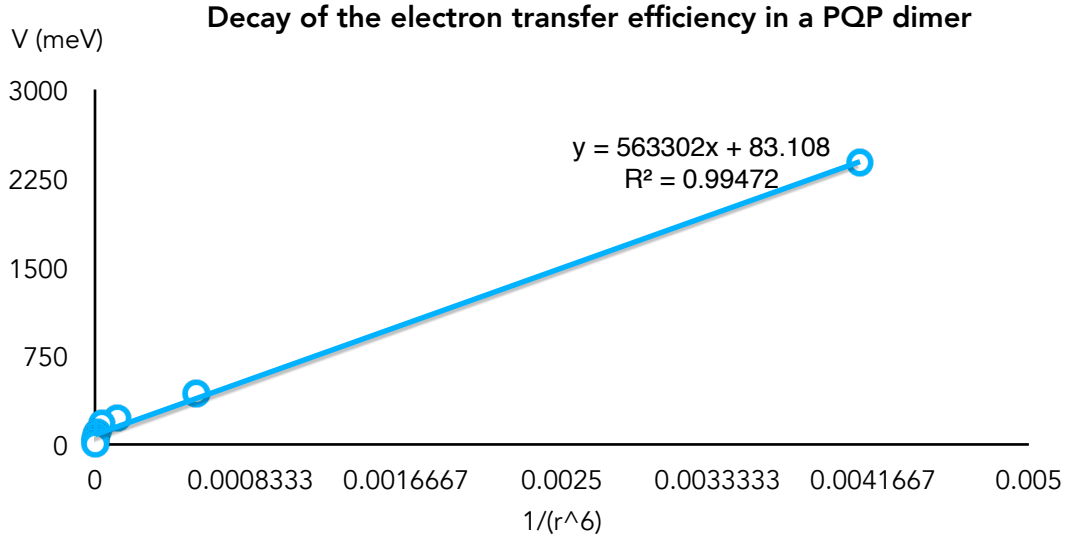

Figure 22. Fitting to r^{-6} of the electron transfer decay when the distance of separation between the monomers is increased

Rotations

The V values for the electron transfer when one of the monomers in a PQP dimer is rotated from 0-90° at different distances of separation are depicted in Figure 23.

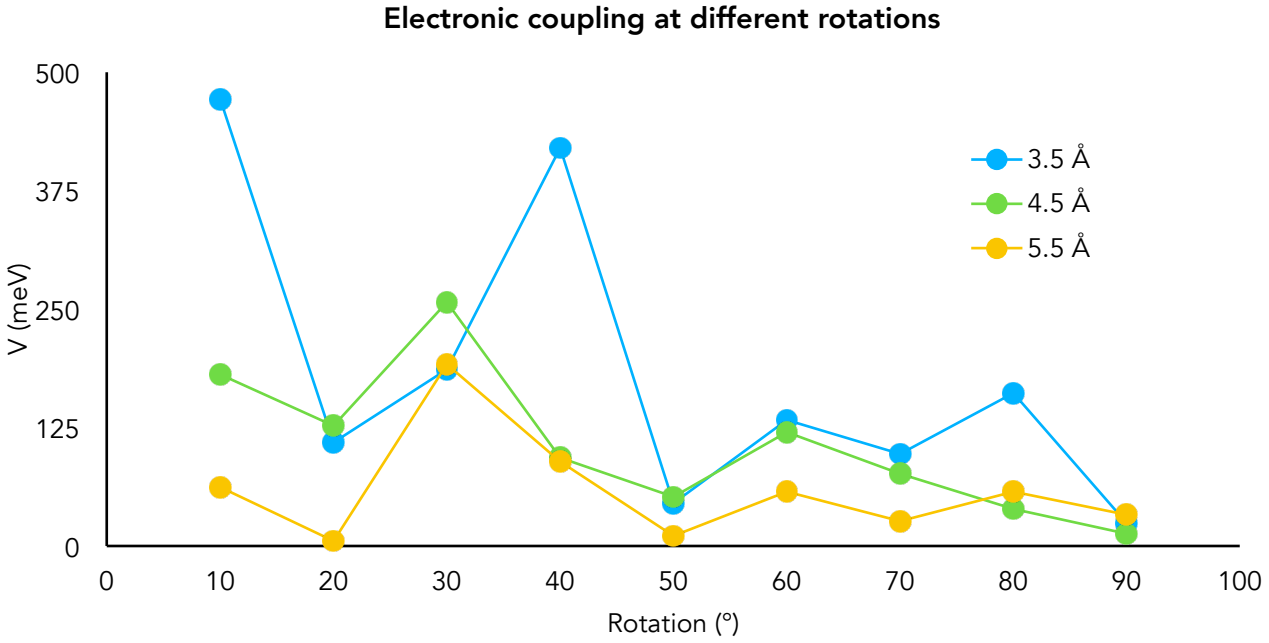

Figure 23. Electronic coupling (electron) when one of the monomers is rotated along its long molecular axis in a PQP dimer at three different distance of separation

The orbital overlap between the LUMO of the cation with the LUMO of the neutral form was obtained to explain the difference of V values at different rotations; the values are depicted in Figure 24.

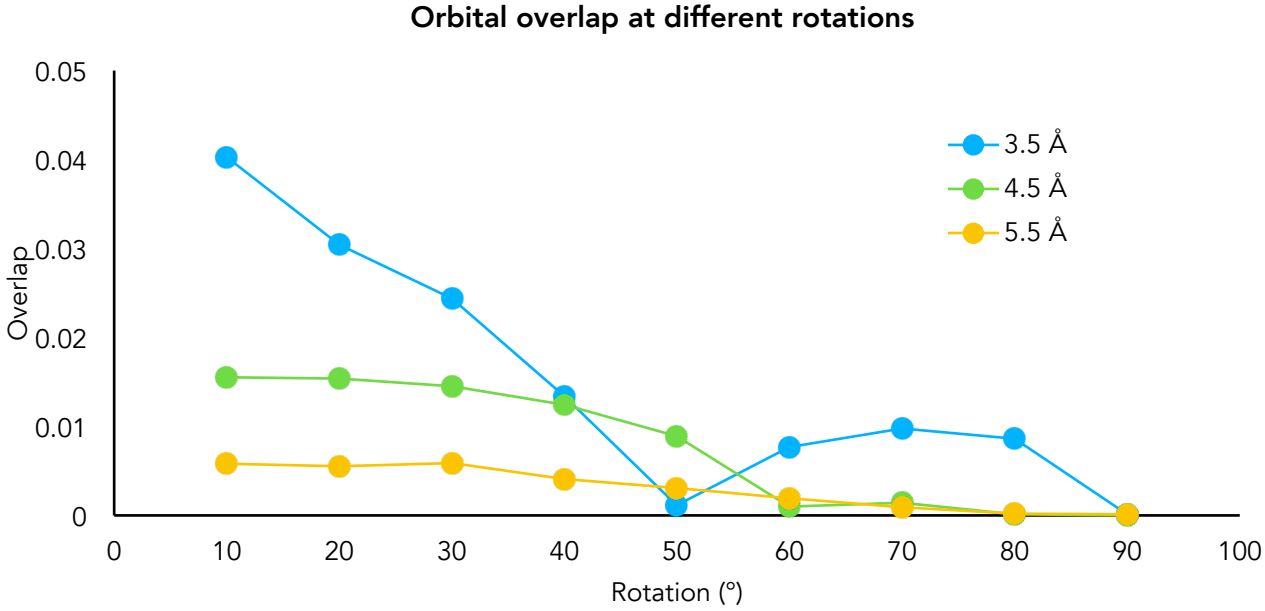

Figure 24. Orbital overlap between the LUMO of the cation and the LUMO in the neutral form when one of the monomers is rotated along its long molecular axis in a PQP dimer at three distances of separation

From Figure 23 it can be observed that for the three distances of separation studied, the electron transfer is not enhanced for most of the configurations, the only exception for both cases is when the monomer rotates 30°, in this case there is a slightly increasing in the V value due to a higher overlap of the LUMOs, for example, at 5.5 Å the LUMO overlap at 20° is 0.0055 but when it is rotated to 30° the overlap increases up to 0.0059. In the case of all distances of separation studied, the rotations do not enhance the electron transfer when compared with the initial (cofacial) configuration; therefore the liquid phase (in which all rotations are allowed) is expected to not transfer electrons.

Displacements

Unlike the effect of rotating a monomer, in which there is a correspondence between the LUMO overlap of the monomers and the V value, during the displacement the electronic coupling does not match entirely with the orbital overlap, i.e. the highest orbital overlap does not always correspond to the highest V. From Figure 25, it could be inferred initially that highest V values correspond to the 4, 5 and 9 Å displacements at a distance of separation of 3.5 Å, since in these configurations the highest LUMO overlap is observed.

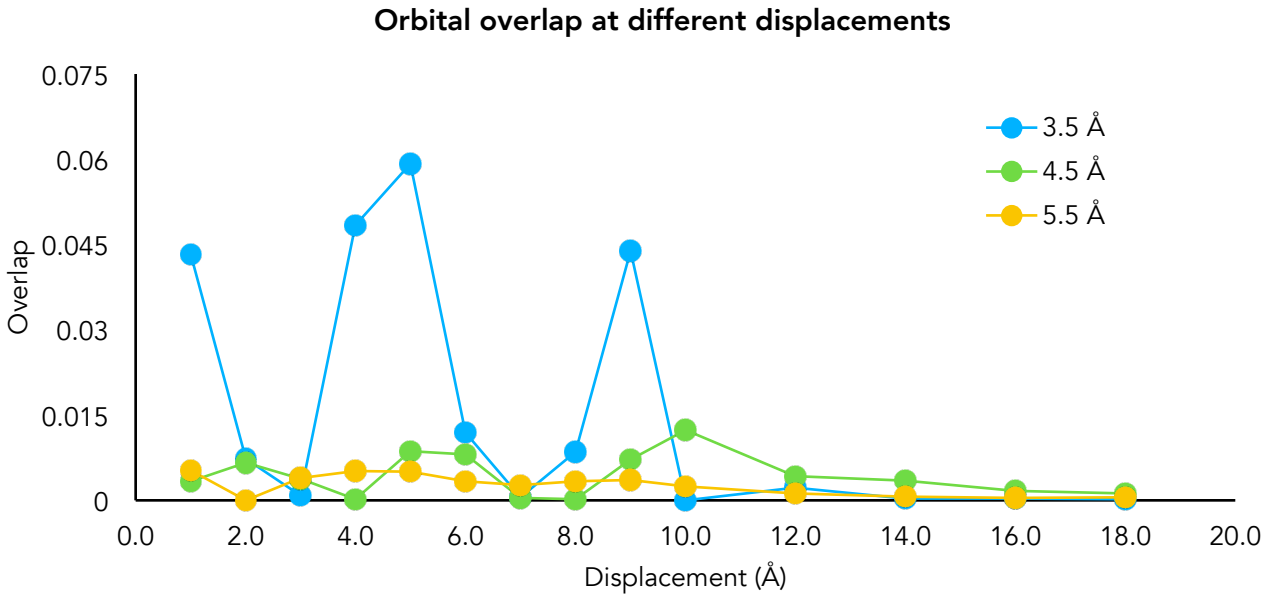

Figure 25. Orbital overlap between the LUMO of monomer A with LUMO in monomer B at different rotations of one of the monomers in a PQP dimer at three different distances of separation

Nevertheless, the highest V values observed in distance of separation of 3.5 Å are at 4 and 9 Å (Figure 26) only, and the displacement at 5 Å shows a small V value. It is worth to mention that for the other two distances of separation studied, there is no a significant enhancement of the electron transfer when one of the monomers is displaced. Actually, when the distance between the monomers is 5.5 Å the V practically is 0, indicating that at this distance of separation there is no electron transfer between the units. For the case of 4.5 Å, even tough some configurations seem to enhance the electron transfer (displacements of 2,0 and 6,0 Å) this is small compared with the initial cofacial configuration.

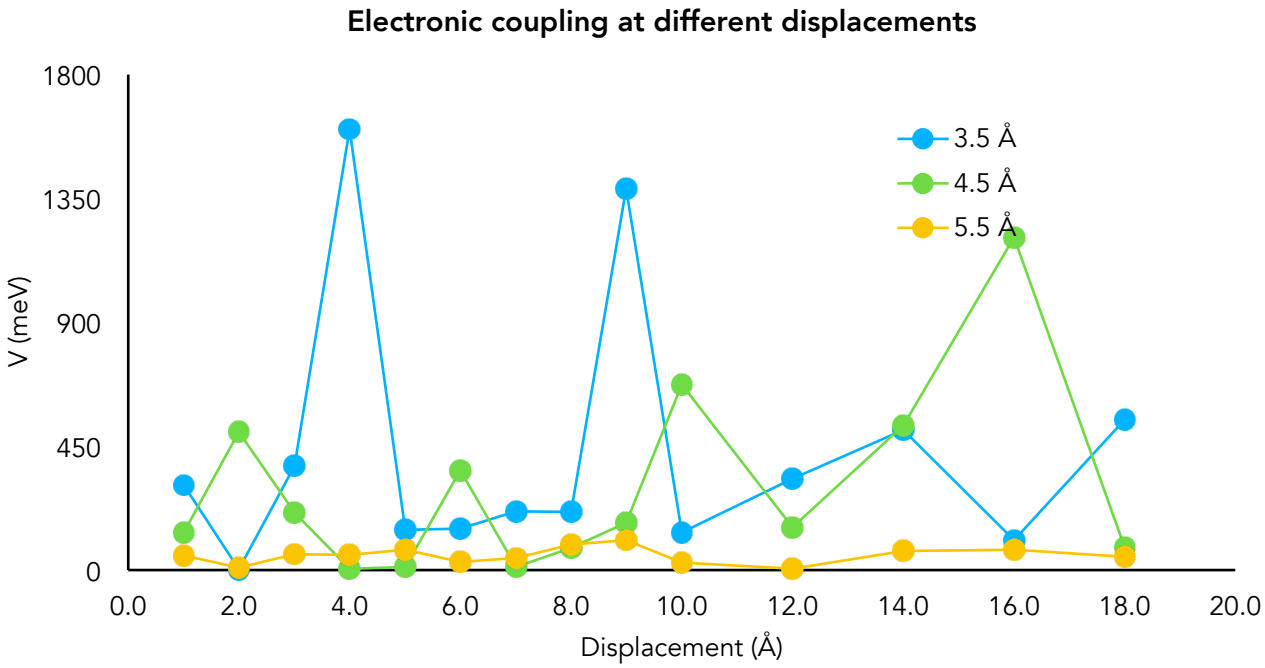

Figure 26. Electronic coupling (electron) at different displacements of one monomer in a PQP dimer at three distances of separation

The total charge (Q) of each ring in the PQP anion was obtained from the individual Mulliken charges to explain the high V clause at a displacement of 4 Å, and the results are shown in Table 5.

Table 5. Total charges of the anionic form of PQP per ring

Number ring	Q
1	-0.112
2	-0.207
3	**-0.353**
4	-0.197
5	-0.125

Further investigation it has been done to understand the small electronic coupling at the displacement of 5 Å. Nevertheless, from the results it can be concluded that the parallel displacements at any distance of separation do not enhance the electron transfer. Therefore, the liquid crystalline phase of PQP is not expected to be an electron transporter.

Conclusions and outlook

The PQP is preferably a hole conductor in most of the configurations in the liquid crystalline phase. High electronic coupling values arise from the parallel displacements of the molecules; these movements are exclusively allowed in the liquid crystalline phase of *p*-quinquephenyl. The rotations of the monomers are limited in this phase due to the short distances of separation (3.5 - 5.5 Å), and therefore do not contribute to the hole transfer. In comparison with the crystal (V = 150 meV), the hole transfer is enhanced in the liquid crystalline phase. The low electronic coupling values obtained for the different displacements and rotations for the electron transfer suggest that the liquid crystalline phase is not suitable for transferring electrons. The results of this work indicate that PQP is a material with a high hole mobility that could be used in liquid crystalline-based electronic devices.

For the liquid phase of PQP, charge transfer (electron and hole) is not expected to occur due to the low electronic couplings at high distances of separation between the molecules (> 6.0 Å) and the free rotations of the monomers.

Currently, the influence of including the relaxed structure of the cation and the anion is being explored to determine if there is any difference with the non-relaxed calculations, and if then the relaxed structures are necessary for the proper description of the dimer. Further research is needed to explore the influence that another PQP monomer has in the charge transfer between two units, as well as the influence of more monomers. Besides the study of the effect of the surroundings, the material can be explored for exciton transfer using the same methodology described in this work.

References

1. Wilson, J., J.F.B. Hawkes, and J.J. Faris, *Optoelectronics: An Introduction.* American Journal of Physics, 1984. **52**(5): p. 479-479.
2. Lagerwall, J.P.F. and G. Scalia, *A new era for liquid crystal research: Applications of liquid crystals in soft matter nano-, bio- and microtechnology.* Current Applied Physics, 2012. **12**(6): p. 1387-1412.
3. J. L. Bredas, J.P.C., D. A. da Silva Filho, and J. Cornil, *Organic semiconductors: A theoretical characterization of the basic parameters governing charge transport.* PNAS, 2002. **99**(9): p. 5804-5809.
4. Wang, C., et al., *Semiconducting pi-conjugated systems in field-effect transistors: a material odyssey of organic electronics.* Chem Rev, 2012. **112**(4): p. 2208-67.
5. Geoffrey R. Hutchison, M.A.R., and Tobin J. Marks, *Intermolecular Charge Transfer between Heterocyclic Oligomers. Effects of Heteroatom and Molecular Packing on Hopping Transport in Organic Semiconductors.* J. Am. Chem. Soc. , 2005. **127**: p. 16866-16881.
6. Yasuhiko Shirota, a.H.K., *Charge Carrier Transporting Molecular Materials and Their Applications in Devices.* Chem. Rev. , 2007. **107**: p. 953-1010.
7. Marcus, R.A., *Electron Transfer reactions in chemistry: Theory and experiment.* Journal of Electroanalytical Chemistry, 1997. **438**: p. 251-259.
8. Plasser, F. and H. Lischka, *Analysis of Excitonic and Charge Transfer Interactions from Quantum Chemical Calculations.* J Chem Theory Comput, 2012. **8**(8): p. 2777-89.
9. Yang, C.H. and C.P. Hsu, *A multi-state fragment charge difference approach for diabatic states in electron transfer: extension and automation.* J Chem Phys, 2013. **139**(15): p. 154104.
10. Van Voorhis, T., et al., *The diabatic picture of electron transfer, reaction barriers, and molecular dynamics.* Annu Rev Phys Chem, 2010. **61**: p. 149-70.
11. Hsu, C.P., *The Electronic Couplings in Electron Transfer and Excitation Energy Transfer.* Accounts of Chemical Research, 2009. **42**(4): p. 509-518.
12. N. Kirova, S.B., A.R. Bishop, *A systematic theory for optical properties of phenylene-based polymers.* Synthetic Metals, 1999. **100**: p. 29-53.
13. You, Z.-Q. and C.-P. Hsu, *Theory and calculation for the electronic coupling in excitation energy transfer.* International Journal of Quantum Chemistry, 2014. **114**(2): p. 102-115.
14. Jean-Luc Bredas, D.B., Veaceslav Coropceanu, and Jerome Cornil, *Charge-Transfer and Energy-Transfer Processes in pi-conjugated Oligomers and Polymers: A molecular picture* Chem. Rev., 2004. **104**: p. 4971-50003.
15. Zhang, Z. and H. Guo, *The phase behavior, structure, and dynamics of rodlike mesogens with various flexibility using dissipative particle dynamics simulation.* J Chem Phys, 2010. **133**(14): p. 144911.
16. Vita, F., et al., *Molecular ordering in the high-temperature nematic phase of an all-aromatic liquid crystal.* Soft Matter, 2016. **12**(8): p. 2309-14.
17. Kuiper, S., et al., *Elucidation of the orientational order and the phase diagram of p-quinquephenyl.* J Phys Chem B, 2011. **115**(6): p. 1416-21.
18. K. N. Baker, A.V.F., T. Resch, H. C. Knachel, *Crystal structures, phase transitions and energy calculations of poly(p-phenylene) oligomers.* Polymer Papers, 1993. **34**(8): p. 1571-1587.
19. P. A. Irvine, D.C.W., P. J. Flory, *Liquid-crystalline Transitions in Homologous p-Phenylenes and their Mixtures.* J. Chem. Soc. Faraday Trans. 1, 1984. **80**: p. 1795-1806.

20. P. J. Flory, P.A.I., *Liquid-crystalline Transitions in Homologous p-Phenylenes and their Mixtures. Part 2: Theoretical Treatment.* J. Chem. Soc. Faraday Trans. 1, 1984. **80**: p. 1807-1819.
21. Y. Olivier, L.M., C. Zannoni, *Quinquephenyl: the simplest rigid rod-like nematic liquid crystal. Or is it? An atomistic simulation.* ChemPhysChem, 2014. **15**: p. 1345-1355.
22. Ma, D., G. Li Manni, and L. Gagliardi, *The generalized active space concept in multiconfigurational self-consistent field methods.* J Chem Phys, 2011. **135**(4): p. 044128.
23. Olsen, J., *The CASSCF method: A perspective and commentary.* International Journal of Quantum Chemistry, 2011. **111**(13): p. 3267-3272.
24. Havenith, R.W.A., H.D. de Gier, and R. Broer, *Explorative computational study of the singlet fission process.* Molecular Physics, 2012. **110**(19-20): p. 2445-2454.
25. Stoyanova, A., et al., *Hopping matrix elements from first-principles studies of overlapping fragments: Double exchange parameters in manganites.* International Journal of Quantum Chemistry, 2006. **106**(12): p. 2444-2457.
26. F. Aquilante, L.D.V., N. Ferré, G. Ghigo, P.-Å. Malmqvist, P. Neogrády, T.B. Pedersen, M. Pitonak, M. Reiher, B.O. Roos, L. Serrano-Andrés, M. Urban, V. Veryazov, R. Lindh, *MOLCAS 7: the next generation.* Journal of Computational Chemistry,, 2010. **31**: p. 224-247.
27. Canola, S., C. Pecoraro, and F. Negri, *Dimer and cluster approach for the evaluation of electronic couplings governing charge transport: Application to two pentacene polymorphs.* Chemical Physics, 2016. **478**: p. 130-138.